Conversations in the tumor microenvironmentasion: experimental models of fibroblast driven cancer cell inv

Mehta; P.P.

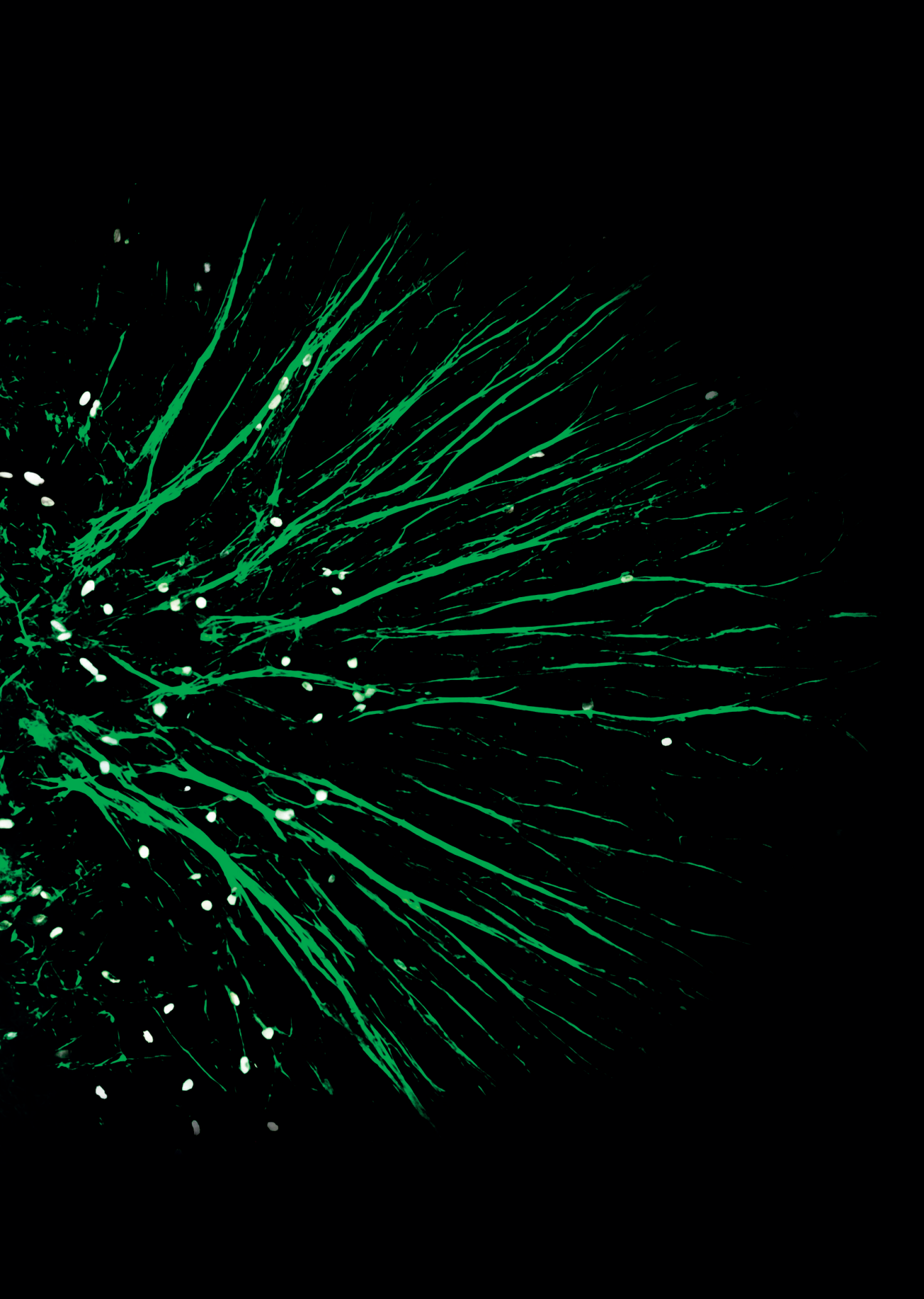

Chapter 4

Hidden TGF-β signaling in fibroblast lung cancer crosstalk

Conditioned medium (CM) induces dissemination of lung adenocarcinoma spheroids via receptor signaling without measurable TGF-β ligand

Pranav Mehta[a,b], Zaid Rahman[b], Ankit Sinha[b], Kristen David[b], Gerard van der Zon[a], Pouyan E. Boukany[b], Peter ten Dijke[a]

[a]Department of Cell and Chemical Biology and Oncode Institute, Leiden University Medical Center, Leiden, the Netherlands
[b]Department of Chemical Engineering, Delft University of Technology, Van der Maasweg 9, 2629 HZ, Delft, the Netherlands

Abstract

Paracrine signaling from stromal fibroblasts is a key regulator of lung cancer invasion, but its signaling requirements in three-dimensional (3D) matrices are incompletely defined. In this chapter, we examined the effect of lung fibroblast–derived CM on A549 lung adenocarcinoma spheroids embedded in GelMA hydrogels. MRC5 CM induced pronounced single-cell dissemination from A549 spheroids in compliant (3% w/v) matrices, while control spheroids remained compact and viable. Dissemination was completely abolished by inhibition of TGF-β type I receptors (ALK4/5) using SB-431542 and significantly reduced by pan–TGF-β neutralization, whereas fibroblast-induced spheroid expansion was suppressed only by ALK4/5 inhibition. Reporter assays and sensitive detection approaches showed no detectable active or total soluble TGF-β in MRC5 CM. Together, these results demonstrate that fibroblast-CM promotes single-cell dissemination of lung adenocarcinoma spheroids through a requirement for ALK4/5 signaling, despite the absence of detectable soluble TGF-β in the CM.

Keywords: lung cancer; TGF-β; Conditioned medium; cancer cell invasion; GelMA

Introduction

Lung cancer remains a major contributor to global cancer-related mortality, with non–small cell lung cancer (NSCLC) representing the majority of diagnoses and characterized by early and aggressive metastatic behavior [1]. Increasing evidence shows that tumor progression is not dictated solely by cancer cell–intrinsic programs but emerges from reciprocal signaling with the tumor microenvironment, particularly with stromal fibroblasts. Through extracellular matrix remodelin, secretion of soluble factors, and modulation of tissue mechanics, these fibroblasts in close proximity of cancer cells can reprogramme cancer cells toward invasive phenotypes. These stromal cues have been implicated in promoting epithelial–mesenchymal transition (EMT), single-cell dissemination, and enhancing metastatic potential across multiple solid tumors [2].

Among the signaling pathways mediating fibroblast–tumor crosstalk, TGF-β has a central and context-dependent role in lung cancer progression, where it promotes EMT, cytoskeletal remodelin, and invasion at advanced disease stages [3]. TGF-β is structurally and functionally related to activin, which signal via type I receptors of the activin receptor-like kinase (ALK)5 and ALK4, respectively. Activated ALK4 and -5 phosphorylate SMAD2/3 to drive transcriptional programmes associated with invasion and EMT. Pharmacological inhibition of these receptors using the small-molecule inhibitor SB-431542 provides a widely used approach to functionally investigate pathway dependence by blocking ALK4/5 kinase activity and therefore, further downstream SMAD signaling [4]. Importantly, inhibition of ALK4 and -5 defines a dependence on ALK4/5-mediated signaling rather than on a specific ligand [4].

In three-dimensional (3D) culture systems, the relationship between paracrine signaling, matrix properties, and invasive behavior is further complicated by spatial confinement, mechanical resistance, and local signal amplification. Under these conditions, functional activation of signaling pathways can occur in the absence of robust bulk readouts of soluble ligand, challenging ligand-centric interpretations of paracrine control. As a result, receptor-level perturbation provides a critical tool for defining signaling dependencies in matrix-embedded tumor models.

Here, we investigated the MRC5 lung fibroblast CM-induced dissemination of A549 lung adenocarcinoma cells using a 3D GelMA spheroid model. Invasive response of A549 cells upon MRC5 CM stimulation was abolished by inhibition of ALK4/5 signaling using a small molecule kinase inhibitor and significantly attenuated by neutralization of TGF-β activity, despite the absence of detectable soluble TGF-β in the CM. By combining live-cell imaging with quantitative invasion and reporter assays, this study defines a fibroblast-driven, TGF-β type I receptor-like-dependent signaling axis that promotes early single-cell dissemination in a 3D lung cancer model.

Methods

Cell Culture

Wild-type A549 human male lung adenocarcinoma cells (CCL-185, ATCC) and MRC-5 lung fibroblasts (CCL-171, ATCC) were obtained from ATCC. A549-VIM-RFP–CAGA12-GFP dual reporter cells were kindly provided by Yifan Zhu (Department of Cell and Chemical Biology, LUMC) [5]. The CAGA12-GFP reporter system has been functionally validated in multiple independent studies [6], [7]. Human hepatocellular carcinoma HepG2 cells (HB-8065™, ATCC) were obtained from ATCC and stably transduced to express the $CAGA_{12}$-GFP reporter as previously described[7]. All cell lines were cultured in DMEM (Gibco, #41965039) supplemented with 10% FBS (Gibco) and 1% Antibiotic–Antimycotic solution (Gibco) under standard conditions (37 °C, 5% CO_2). Cells were used between passages 5 and 15, routinely passaged at 80–90% confluency, sub-cultured two to three times per week, regularly screened for mycoplasma contamination, and authenticated by STR profiling.

A549 Spheroid Generation

A549 spheroids were generated in Corning™ Elplasia™ 96-well round-bottom plates with an ultra-low attachment (ULA) surface (Corning) to prevent cell–substrate adhesion and promote cell–cell aggregation. Wells contained 79 micro-wells, each seeded at 500 cells (total 4.0 x 10^4 cells per well). Spheroids were cultured for 4 days to a mean diameter of 200 ± 30 µm before use[8].

Generation of MRC5 CM

1x10^5 MRC-5 fibroblasts were seeded per well in 12-well plates and maintained for 3 days in standard culture medium as mentioned above in subsection 2.1. The CM was then collected, and passed through a 0.45 µm filter to remove cell debris. This CM was used immediately, either undiluted or diluted with standard culture medium for stimulation experiments.

Preparation and cross-linking of GelMA hydrogels

Gelatin methacryloyl (GelMA; 300 g bloom, ~60% degree of substitution; Sigma-Aldrich) was prepared at 3% or 5% (w/v) in Dulbecco's phosphate-buffered saline (DPBS; Gibco) with lithium phenyl-2,4,6-trimethylbenzoylphosphinate (LAP; Sigma-Aldrich) at a LAP:GelMA mass ratio of 1:16. Solutions were incubated at 37°C in a water bath for ~2 h until fully dissolved. Hydrogels were cross-linked by exposure to 365 nm UV light (Spectroline, serial no. 1832066) for 45s.

Invasion Assays

A549 spheroids were suspended in 3% (w/v) GelMA and polymerized in Ibidi 8-well µ-Slides as described above. Each hydrogel was overlaid with 200 µL culture medium and imaged using a Zeiss LSM 980 confocal microscope equipped with a live-cell incubation chamber (37 °C, 5% CO_2). Medium was refreshed every 48 hours. Images were acquired at 24 hour intervals. Brightfield images were acquired using transmitted light (TL) illumination on the Zeiss LSM 980. The transmitted light was detected using the transmitted photomultiplier tube (TPMT) detector and master gain was set to 350V, digital gain set to 1.0 and digital offset to 0. Green fluorescence protein (GFP) images were acquired using an EC Plan-Neofluar 10×/0.3 NA M27 air objective with a 13 mW 488 nm laser (0.2% power, master gain 650 V, digital gain 1, digital offset 0). The field of view was 848.53 x 848.53 μm^2 (2048 × 2048 pixels) at 1.0x optical zoom. Z-stacks were collected at 20 µm steps over a 400 µm range.

Image analysis

Spheroid area was quantified on day 0 and day 7 using ImageJ2 (v2.14, NIH). Maximum-intensity Z-projections were generated, and spheroid boundaries were manually outlined to measure projected area. Spheroid expansion was expressed as the ratio of day 7 to day 0 area. Disseminated single cells were manually counted in the same projections at both time points.

Pharmacological and antibody treatments

Recombinant TGF-β3 (R&D Systems, 7666; Minneapolis, MN, USA) was prepared in 4 mM HCl containing 0.1% recombinant bovine serum albumin (BSA) and used at a final concentration of 1 ng/mL unless stated otherwise. For TGF-β receptor inhibition, spheroids were pre-treated with SB-431542 (10 µM; Sigma-Aldrich) for 1 hour before imaging. For TGF-β ligand neutralization, MRC5 CM was incubated for 30 min at room temperature with the pan-TGF-β neutralizing antibody 1D11 (10 µg/mL; R&D Systems) or its isotype-matched negative control 13C4 at the same concentration, before addition to spheroid cultures.

CAGA12-GFP reporter & 2D TGF-βassay

To assess TGF-β levels in fibroblast-derived conditioned medium, HepG2 CAGA12-GFP reporter cells were seeded in 96-well plates (#3595, Corning) and exposed to graded concentrations of recombinant TGF-β3 or MRC5 conditioned medium. Live-cell imaging was performed at 2-hour intervals using the Incucyte® S3 system with brightfield and GFP fluorescence acquisition (488 nm laser, 300 ms exposure). Fluorescence intensity and cell confluency were quantified using Incucyte® S3 software, with data pooled from three independent wells. Signal-to-background (s/b) values were calculated by normalizing

fluorescence intensity to unstimulated controls at corresponding time points. Z′ scores were calculated using the following formula:

$$Z' = \frac{3 \times (STDev_{pos} + STDev_{neg})}{|AVG_{pos} - AVG_{neg}|}$$

For the fluorescence reporter assay, A549 $CAGA_{12}$–GFP cells ($1x10^5$ per well) were seeded in 12-well plates and incubated overnight to allow adhesion. The following day, cells were washed with PBS and stimulated with either recombinant TGF-β1 (10 ng/mL) or MRC5 CM in a total volume of 1.5 mL culture medium per well.

Graphing and Statistical Analysis

All data were analyzed and plotted in GraphPad Prism (v10, GraphPad Software). Results are presented as mean ± SD from ≥3 independent experiments unless stated otherwise. Comparisons were performed using two-way ANOVA with post hoc tests or nonparametric t tests as appropriate. *P* values < 0.05 were considered significant.

Results

MRC5 CM induces single-cell dissemination of A549 CAGA–GFP cells in 3D GelMA matrices

A549 $CAGA_{12}$–GFP reporter cells embedded in 3% (w/v) GelMA hydrogels exhibited uniform spheroid expansion over 7 days in control medium, with no detectable dissemination (Fig. 1A). In contrast, exposure to 100% CM derived from MRC5 lung fibroblasts induced a pronounced single-cell dissemination phenotype, characterized by numerous cells migrating away from the spheroid core into the surrounding matrix (Fig. 1A, MRC5 CM). Quantification revealed a significant increase in disseminated single cells in CM-treated cultures compared with control ($P < 0.001$; Fig. 1B). Spheroid expansion, assessed as the ratio of spheroid area at day 7 to day 0, was modestly increased in CM relative to control ($P > 0.05$; Fig. 1C).

The magnitude of dissemination depended on the concentration of fibroblast-derived CM. Treatment with 10% MRC5 CM had no measurable effect on dissemination or spheroid expansion (Supporting Fig. 1). Increasing CM concentration to 30% induced limited single-cell dissemination by day 5, which remained difficult to quantify due to the early stage of migration (Supporting Fig. 2). Thus to enable robust and reproducible quantification of dissemination, all subsequent experiments were therefore performed using 100% MRC5 CM. Matrix composition further modulated response to fibroblast signals. When A549 spheroids were cultured in a stiffer 5% (w/v) GelMA matrix, MRC5 CM promoted spheroid expansion and compaction but failed to induce single-cell dissemination over the same

time frame (Supporting Fig. S3). Based on these observations, 3% (w/v) GelMA was selected as a permissive matrix condition for analysing fibroblast-induced dissemination.

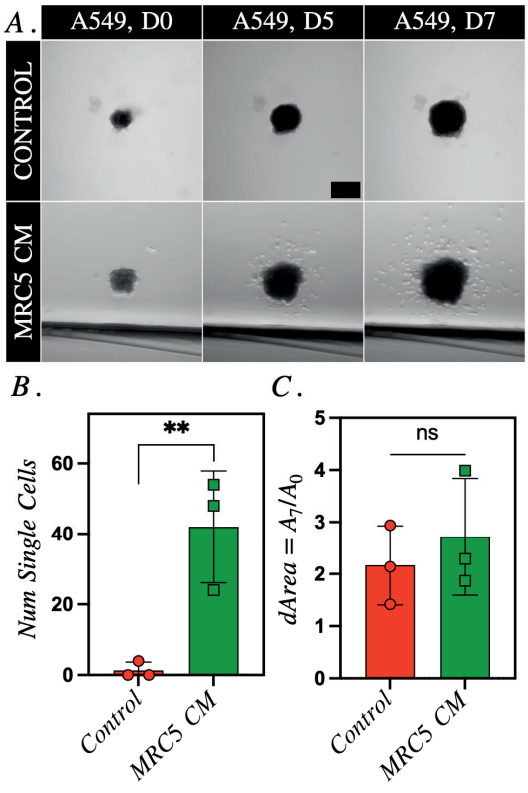

Figure 1. MRC5 CM induces single-cell dissemination in A549 spheroids embedded in 3% (w/v) GelMA.

A. Brightfield maximum-projection images (Day 0, Day 5 and, Day 7) of A549 spheroids cultured in control medium or MRC5 CM. Spheroids increased in size under both conditions; however, CM stimulation induced numerous rounded single cells migrating away from the spheroid by Day 7. Scale Bar = 200 µm.

*B. Quantification of single cells per condition. Data represents mean ± SD (control: 1 ± 2.3, CM: 42 ± 16, n = 3 biological replicates, ≥ 2 technical repeats each). **P < 0.01, two-tailed unpaired t-test.*

C. Spheroid expansion over 7 days, expressed as the ratio of spheroid area at Day 7 to Day 0. Data represents mean ± SD (control: 2.2 ± 0.8, CM: 2.9 ± 1.1, n = 3 biological replicates, ≥ 2 technical repeats each). P > 0.05, two-tailed unpaired t-test.

TGF-β type I receptor inhibition abolishes fibroblast-induced dissemination

CM-induced dissemination was abolished upon pharmacological inhibition of TGF-β type I receptor activity using SB-431542, restoring a compact spheroid morphology (Fig. 2A, CM + SB). Disseminated cell counts in the SB + CM group were reduced to baseline control levels ($P < 0.0001$ vs CM alone; Fig. 2B). In addition to suppressing dissemination, SB-431542 treatment also reduced spheroid expansion to levels significantly below those observed in control cultures, indicating an additional suppressive effect on spheroid growth (Fig. 2C) [9].

To assess whether dissemination was driven by TGF-β activity in the CM, CM was treated with the pan–TGF-β–blocking antibody 1D11, a potent inhibitor of all three isoforms[10]. 1D11 treatment significantly reduced single cell dissemination to a similar extent as SB-431542 ($P < 0.001$ vs CM; Fig. 2B) but had little effect on spheroid expansion, which remained comparable to untreated CM ($P > 0.05$; Fig. 2C). These results indicate that dissemination in this model is dependent on TGF-β receptor signaling, whereas fibroblast-driven spheroid expansion is largely TGF-β–independent.

Absence of detectable TGF-β ligand in MRC5-CM

To test for the presence of soluble TGF-β activity, A549 $CAGA_{12}$–GFP reporter cells were stimulated with TGF-β3 (10 ng/mL) ligand or MRC5 CM, followed by quantification of GFP signal after 18 hours. TGF-β3 stimulation induced a robust increase in reporter intensity, whereas CM elicited no change relative to control (Fig. 3A).

To further assess the presence of soluble TGF-β activity, active and total TGF-β3 levels in MRC5 CM were measured using a high-sensitivity reporter assay, with HepG2 $CAGA_{12}$–GFP reporter cells used as positive controls. Neither active nor total TGF-β3 was detected above the assay's lower limit in CM, whereas recombinant TGF-β3 at concentrations as low as 0.05 ng/mL produced a clear reporter response (Fig. 3B). Together, these data demonstrate that fibroblast-CM promotes single-cell dissemination through a TGF-β type I receptor-like -dependent signaling requirement that occurs in the absence of detectable soluble TGF-β3.

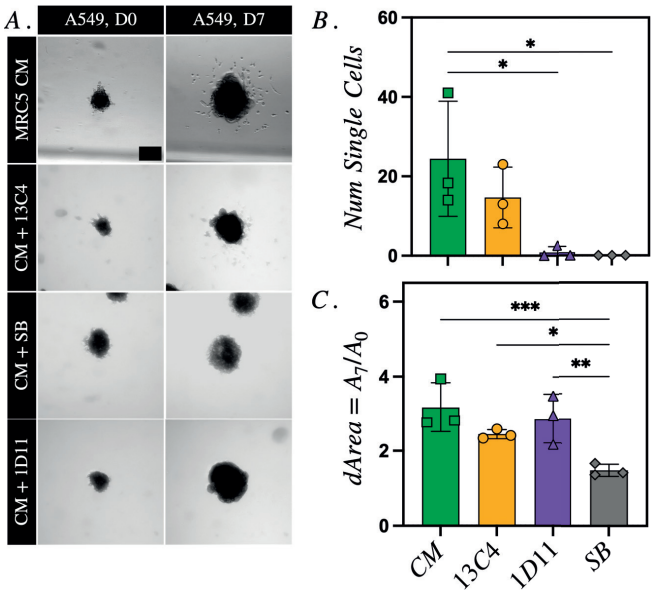

Figure 2. TGF-β and TGF-B type I receptor inhibition prevents single-cell dissemination in A549 spheroids.

A. Brightfield maximum-projection images (Day 0 and Day 7) of A549 spheroids cultured in control medium or MRC5 CM. CM stimulation increased spheroid size and induced single-cell dissemination, whereas treatment with SB-431452 or neutralization of TGF-β in CM using 1D11 prevented dissemination. Scale Bar = 200 µm.

*B. Quantification of single cells per condition on Day 7. Data represents Mean ± SD (CM: 24 ± 14, 13C4: 15 ± 8, 1D11: 1 ± 1, SB: 0 ± 0, n = 3 biological replicates, ≥2 technical repeats each). *P < 0.05*

*C. Spheroid expansion over 7 days, expressed as the ratio of spheroid area at Day 7 to Day 0. Data represents Mean ± SD (CM: 3.2 ± 0.7, 13C4: 2.4 ± 0.1, 1D11: 2.9 ± 0.7, SB: 1.5 ± 0.1, n = 3 biological replicates, ≥2 technical repeats each. ***P < 0.001, **P < 0.01, *P < 0.05. No statistical significance was found upon comparing CM group to 13C4 and 1D11 groups. Statistical significance was determined by two-way ANOVA (factors: treatment × replicate) with Tukey's post-hoc.*

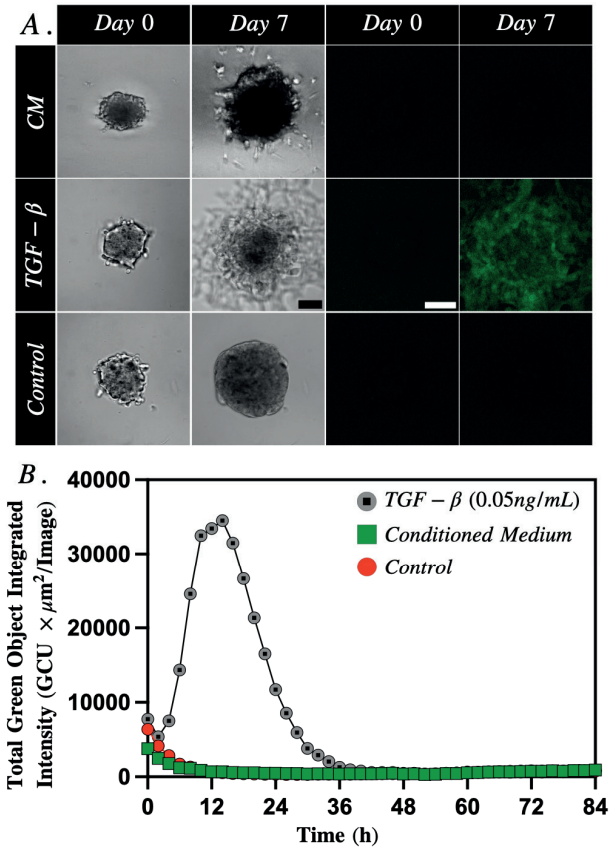

Figure 3. MRC5 CM lacks detectable TGF-β activity.

A. Brightfield and GFP fluorescence images of A549 CAGA–GFP spheroids embedded in 3% (w/v) GelMA on day 0 and day 7 following stimulation with recombinant TGF-β1 or MRC5 CM. TGF-β1 (10 ng/mL) treated spheroids exhibit pronounced invasion and increased GFP reporter activity, whereas control and CM-treated spheroids show minimal changes.

B. Fluorescence reporter assay confirming absence of measurable TGF-β in MRC5 CM, with standard (0.05 ng/mL) producing a robust concentration-dependent signal.

Discussion

Our results demonstrate that CM obtained from MRC5 fibroblasts promotes single-cell dissemination of A549 lung adenocarcinoma spheroids in 3D GelMA matrices, despite the absence of detectable soluble TGF-β in the CM of MRC5 cells. Dissemination was completely abolished by pharmacological inhibition of ALK4/5 signaling using SB-431542 and significantly reduced by neutralization of TGF-β activity with the pan–TGF-β antibody 1D11, whereas fibroblast-driven spheroid expansion was suppressed only by SB-431542.

Together, these findings establish a clear requirement for TGF-β type I receptor like signaling in fibroblast-induced dissemination, while indicating that distinct receptor-dependent mechanisms underlie dissemination and spheroid growth. The ability of TGF-β type I receptor kinase inhibitor and TGF-β neutralizing antibody inhibit A549 spheroid cell invasion induced by MCR5 CM, but the inability to detect soluble TGF-β in CM suggests that dissemination is TGF-β dependent, but is enhanced by other soluble factors that are present in the CM. Our finding that the small molecule ALK4/5 inhibitor, which targets both TGF-β type I and Activin type I receptors, produced a more pronounced inhibition of dissemination than 1D11, which neutralises TGF-β but not activin, suggests that activin signalling from MRC5 CM may contribute to the observed dissemination phenotype. Together, this work reveals that fibroblast-derived paracrine cues can drive early single-cell dissemination of lung adenocarcinoma spheroids through a TGF-β-like dependent signaling in the absence of detectable soluble TGF-β. Further work will be required to define the factors with which TGF-β like signals cooperate to induce A549 cell sphroid invasion.

Several mechanistic explanations may account for TGF-β receptor activation in the absence of detectable soluble ligand. First, TGF-β may be present in the CM at concentrations below the detection threshold of standard assays, yet sufficient to activate receptors under permissive conditions. Second, latent TGF-β complexes may be activated locally at the cell surface through integrin-mediated or protease-mediated mechanisms, bypassing the need for freely diffusible active ligand[11], [12]. Third, other ALK4/5 ligands present in fibroblast CM, including activins and Growth Differentiation Factor (GDF) family members, may activate overlapping downstream signalling cascades, consistent with the more pronounced inhibition observed with SB-431542 compared to the TGF-β-specific antibody 1D11 [13]. Finally, crosstalk from integrin-FAK or other mechanosensing pathways may transactivate Smad-dependent signalling independently of canonical ligand-receptor engagement [14]. Distinguishing between these possibilities will require proteomic characterisation of the MRC5 secretome combined with targeted ligand depletion and phosphoproteomic approaches.

Supporting Figures

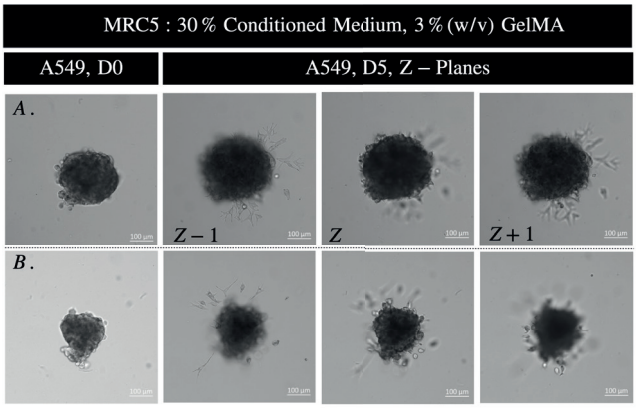

Supporting Figure 1. *A549 spheroids embedded in 3% GelMA (w/v) displaying no invasive activity on Day 5 after stimulation with 10% MRC5 CM. Yellow and Red circles highlight respective spheroids on Day 0 and Day 5.*

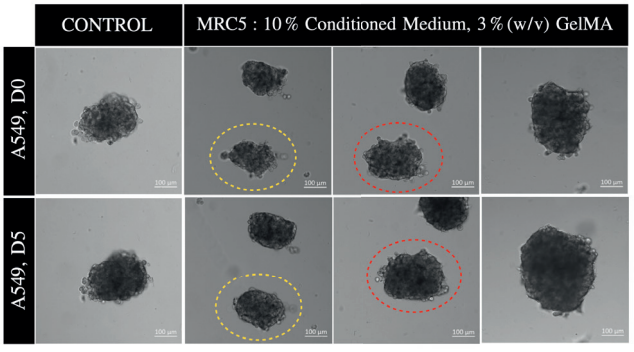

Supporting Figure 2. ***(A) & (B)*** *Multiple Z-planes of A549 spheroids embedded in 3% GelMA (w/v) displaying invasive activity on Day 5 after stimulation with 30% MRC5 CM. Manual quantification revealed, on average, 9 cells beginning to disseminate away from the spheroid in both (A) and (B) by end of Day 5.*

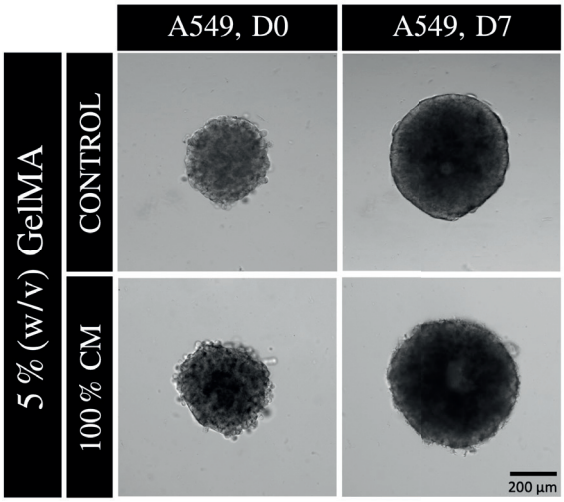

Supporting Figure 3. *A549 spheroids in 5% GelMA (w/v) showing no invasion upon stimulation with 100% MRC5 CM after 7 days.*

References

[1] L. E. L. Hendriks *et al.*, "Non-small-cell lung cancer," *Nat Rev Dis Primers*, vol. 10, no. 1, p. 71, Sep. 2024, doi: 10.1038/s41572-024-00551-9.

[2] R. M. Bremnes *et al.*, "The Role of Tumor Stroma in Cancer Progression and Prognosis: Emphasis on Carcinoma-Associated Fibroblasts and Non-small Cell Lung Cancer," *Journal of Thoracic Oncology*, vol. 6, no. 1, pp. 209–217, Jan. 2011, doi: 10.1097/JTO.0B013E3181F8A1BD.

[3] M. Pickup, S. Novitskiy, and H. L. Moses, "The roles of TGFβ in the tumour microenvironment," *Nature Reviews Cancer*, vol. 13, no. 11, pp. 788–799, 2013, doi: 10.1038/nrc3603.

[4] C. H. Heldin, K. Miyazono, and P. Ten Dijke, "TGF-β signalling from cell membrane to nucleus through SMAD proteins," *Nature*, vol. 390, no. 6659, pp. 465–471, 1997, doi: 10.1038/37284.

[5] W. Wang *et al.*, "Live-cell imaging and analysis reveal cell phenotypic transition dynamics inherently missing in snapshot data," *Science Advances*, vol. 6, no. 36, p. eaba9319, Sep. 2020, doi: 10.1126/sciadv.aba9319.

[6] J. Zhang, M. Thorikay, G. van der Zon, M. van Dinther, and P. ten Dijke, "Studying TGF-β Signaling and TGF-β-induced Epithelial-to-mesenchymal Transition in Breast Cancer and Normal Cells," *Journal of Visualized Experiments (JoVE)*, no. 164, p. e61830, Oct. 2020, doi: 10.3791/61830.

[7] D. L. Marvin *et al.*, "Dynamic Visualization of TGF-β/SMAD3 Transcriptional Responses in Single Living Cells," *Cancers*, vol. 14, no. 10, Art. no. 10, Jan. 2022, doi: 10.3390/cancers14102508.

[8] A. van der Net *et al.*, "EMT-related cell-matrix interactions are linked to states of cell unjamming in cancer spheroid invasion," *iScience*, vol. 27, no. 12, pp. 111424–111424, Dec. 2024, doi: 10.1016/J.ISCI.2024.111424.

[9] S. K. Halder, R. D. Beauchamp, and P. K. Datta, "A Specific Inhibitor of TGF-β Receptor Kinase, SB-431542, as a Potent Antitumor Agent for Human Cancers," *Neoplasia*, vol. 7, no. 5, pp. 509–521, May 2005, doi: 10.1593/neo.04640.

[10] J. R. Dasch, D. R. Pace, W. Waegell, D. Inenaga, and L. Ellingsworth, "Monoclonal antibodies recognizing transforming growth factor-beta. Bioactivity neutralization and transforming growth factor beta 2 affinity purification," *J Immunol*, vol. 142, no. 5, pp. 1536–1541, Mar. 1989.

[11] J. P. Annes, J. S. Munger, and D. B. Rifkin, "Making sense of latent TGFβ activation," *Journal of Cell Science*, vol. 116, no. 2, pp. 217–224, Jan. 2003, doi: 10.1242/jcs.00229.

[12] M. Shi *et al.*, "Latent TGF-β structure and activation," *Nature*, vol. 474, no. 7351, pp. 343–349, Jun. 2011, doi: 10.1038/nature10152.

[13] H. Loomans and C. Andl, "Intertwining of Activin A and TGFβ Signaling: Dual Roles in Cancer Progression and Cancer Cell Invasion," *Cancers*, vol. 7, no. 1, pp. 70–91, Dec. 2014, doi: 10.3390/cancers7010070.

[14] Z. Zi, D. A. Chapnick, and X. Liu, "Dynamics of TGF-β/Smad signaling," *FEBS Letters*, vol. 586, no. 14, pp. 1921–1928, Jul. 2012, doi: 10.1016/j.febslet.2012.03.063.